ADVANCED MATERIALS
www.advmat.de

CMP Aerogels: Ultrahigh-Surface-Area Carbon-Based Monolithic Materials with Superb Sorption Performance

*Ran Du, Na Zhang, Hua Xu, Nannan Mao, Wenjie Duan, Jinying Wang, Qiuchen Zhao, Zhongfan Liu, and Jin Zhang**

Conjugated microporous polymers (CMPs), a rising star among microporous organic polymers (MOPs) have drawn particular interest in recent years.[1–3] Combining delocalized π-conjugated structures with abundant permanent micropores, CMPs not only inherit the attractive features (e.g., high microporosity, precise chemical structures, and high thermal and physicochemical stabilities) of MOPs,[4–6] but also exhibit extended applications in energy- and optics-related fields.[3,8–10]

However, the synthetic methods of CMPs are quite complicated and the reaction conditions are always rigorous, inevitably raising the production costs and hampering practical applications. The specific surface area (SSA) of CMPs is always lower (typically <1000 m^2 g^{-1})[2,3] than many other MOPs, such as covalent organic frameworks (COFs, up to 3620 m^2 g^{-1})[10] and porous aromatic frameworks (PAFs, up to 2932 m^2 g^{-1}).[11] This might be attributed to enhanced aggregation of polymer chains because of π–π interactions originated from their fully conjugated structures. The low SSA not only renders CMPs at a disadvantage in gas sorption, but also deteriorates their performance in capacitors and catalysis owing to reduced active sites.[2] Additionally, 3D networks of CMPs consist of predominant micropores. These nanosized pores can greatly retard mass transfer, and thereby place a great barrier for applications in high-power capacitors and oil sorption.

In this regard, many elegant strategies have been reported to address these problems. Based on monomer design, utilization of predesigned monomers with an appropriate strut length can finely modulate the pore size and improve the SSA to some extent.[1,12] Aromatic nitriles are capable of creating considerably high-surface-area frameworks (over 2000 m^2 g^{-1}) at high temperatures.[13] By post thermal-treatment, the Brunauer–Emmett–Teller (BET) surface area can also be effectively improved.[14,15] On the other hand, the introduction of nitrogen or metal atoms, by means of either monomer design and post-decoration, can also effectively enhance the gas-adsorption performance of CMPs.[16–18] This is due to the enhanced interactions between adsorbents and gas molecules.[17,18]

However, most methods mentioned above are only suitable for specific cases and complicated organic syntheses are always involved. Some methods only give a limited improvement of the SSA, whereas others may destroy the chemical structures because of harsh treatment conditions. Additionally, the purposefully introduction of relatively larger pores (macro- or mesopores) for mass-transfer enhancement is seldom considered. Hence, up to now the development of a general and effective method for the preparation of high-performance CMP-based materials with ultrahigh SSA and hierarchical pores has still remained a huge challenge.

In the field of metal–organic frameworks (MOFs), Hupp and co-workers have shown greatly improved SSA and microporosity by supercritical drying, a method used currently to avoid structure collapse.[19] Directional freeze drying has also been applied for preparing porous polymers with aligned structures with either water or organic solvents.[20] However, high-performance CMP aerogels derived from special drying have never been reported. On this occasion, we propose the monolithic CMP aerogels as a promising candidate to work with the above challenges, based on common knowledge of gels.[21–26] Firstly, with a monolithic form at a macroscopic size, continuous larger pores (macro- and meso- pores) are always included in the gel matrix.[27] Hence, the hierarchically structured CMP aerogel with all-size pores can acquire an enhanced mass-transfer ability. Secondly, the special drying process, such as freeze drying, can efficiently suppress the aggregation of conjugated polymer chains and thereby materials with enormous SSA are obtained. This is because solvents are removed via a sublimation process, bypassing the gas–liquid phase line, thus minimizing the variation of surface tension before and after drying (**Figure 1**). Thirdly, in principle, this strategy is adaptable to almost all kinds of CMPs with minimal damage to materials. Hence the CMP aerogel may provide an unprecedented opportunity to boost the performance of conventional CMPs materials to a new stage.

The synthetic route of the poly(1,3,5-triethynylbenzene) (PTEB) aerogel is illustrated in **Figure 2**a. With 1,3,5-triethynylbenzene (TEB) as a precursor, diverse acetylene-related reactions allow us to select appropriate conditions to conduct coupling reactions in a simple and mild way. Hay's condition for the Glaser coupling reactions, where the oxygen participates in the reaction process, was selected because it allows an air-atomosphere synthesis.[28] In this way, the PTEB organogel can be easily acquired by mixing monomers and low-cost CuCl catalysts in pyridine followed by standing under mild condition

R. Du, N. Zhang, H. Xu, N. N. Mao, W. J. Duan, J. Y. Wang, Q. C. Zhao, Prof. Z. F. Liu, Prof. J. Zhang
Center for Nanochemistry
Beijing National Laboratory for Molecular Sciences
Key Laboratory for the Physics and Chemistry of Nanodevices
State Key Laboratory for Structural Chemistry of Unstable and Stable Species
College of Chemistry and Molecular Engineering
Peking University
Beijing 100871, PR China
E-mail: jinzhang@pku.edu.cn

DOI: 10.1002/adma.201403058

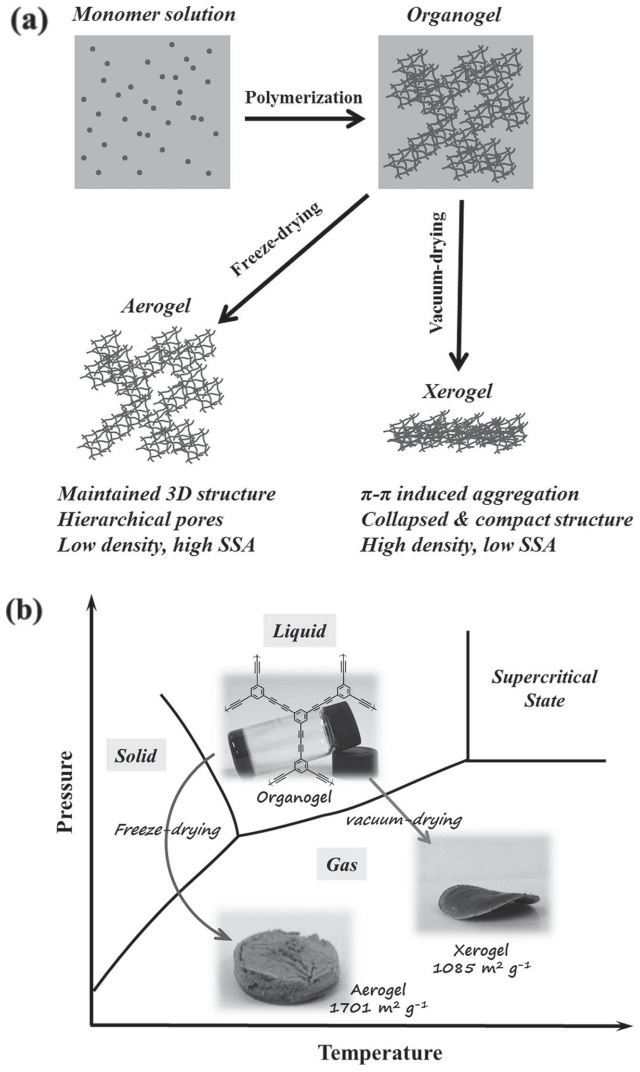

Figure 1. a) Schematic illustration of the structure and preparation procedures for the PTEB aerogel and xerogel. b) Demonstration of monolithic and porous PTEB aerogels acquired from corresponding organogels via freeze-drying, which differs from traditional vacuum drying in avoiding directly crossing the gas–liquid phase line.

(25–60 °C) in air. In comparison with the homocoupling reaction conducted with expensive Pd(II)/CuI catalyst under the protection of inert gas,[17,29,30] the advantages of the current approach are self-evident. These mild conditions, i.e., without the requirement of inert-gas protection and large external energy input, are very competitive for the synthetic process of a number of MOPs. [11,13,31–33]

Bearing three reactive sites, homocoupling of 1,3,5-triethynylbenzene (TEB) under undisturbed conditions resulted in a monolithic 3D network linked by covalent bonds, i.e., a PTEB organogel. In comparison, only precipitates were obtained when bifunctional 1,4-diethynylbenzene (DEB) molecules were used (Figure S1, Supporting Information). It should be noted that, with a limited polymerization degree, the 3D network was actually constructed of combined intramolecular covalent carbon–carbon bonds and intermolecular non-covalent interactions, such as π-π stacking, as shown in Figure 1a, and hence resulted in hierarchical pores in the gel matrix. The wet gels hold a high tolerance to both heat and diverse organic solvents (Figure S2, Supporting Information), facilitating its use in harsh conditions. The insolubility of the PTEB gel in various organic solvents, which is totally different from the TEB monomers, also suggests the formation of well-established 3D networks.[15]

To get more knowledge about the gelation behavior of the TEB, the reaction conditions were systematically investigated by altering the initial monomer concentration (c_0), catalyst amount (w), and reaction temperature (T) (Figure S3, Supporting Information), and a wide gelation window was obtained. The generality of this strategy for the preparation of CMP gels was also demonstrated. For instance, the copolymer gel with a mixture of TEB and DEB as monomers can also be obtained in the same manner (Figure S4, Supporting Information).

After purification and a solvent-exchange process, monolithic PTEB aerogels were obtained from the wet gels by a freeze-drying process with water as the solvent. It should be noted that freeze drying with different solvents may modulate the macropore structure by templating. Elemental analysis (calcd for $C_{12}H_3$: C 97.96, H 2.04, N 0.00; found: C 89.36, H 2.58, N 0.52 at%) and XPS analysis (C 91.43, O 8.57, N 0.00 at%) (Figure S6a,b, Supporting Information) of the products showed a comparable purity to that of CMPs prepared by conventional approaches.[15,34] The slight deviation of the experimental and theoretical results is common for MOPs, and it may be attributed to incomplete polymerization, or adsorption of water or gases during handling.[29,33] The molecular structure of the PTEB aerogel was revealed by spectral methods (Figure S6c,d, Supporting Information). In the Raman spectra, the disappearance of the peak at ca. 2116 cm^{-1} (representing C≡C stretching in the monomers) and the appearance of the new peak at a higher wavenumber (ca. 2221 cm^{-1}, representing the C≡C stretching mode in the phenyl diacetylene) suggested successfully coupling of acetylenic bonds as expected.[34,35] The considerably enhanced broad fluorescence peak may be attributed to the formation of the large conjugated system. The IR spectrum was consistent with that for PTEB reported elsewhere.[29] A significantly reduced intensity ratio of I_{3300}/I_{1572} (the peak at 3300 cm^{-1} represents the ≡C–H vibration and that at 1572 cm^{-1} represents the vibration of the aromatic skeleton), and the shifting of the peak from 2109 cm^{-1} to 2204 cm^{-1} suggested the formation of the targeted products. The peak at ca. 1684 cm^{-1} may be attributed to some side products containing carboxylate groups.

The morphology of the PTEB aerogels was characterized by scanning electron microscopy (SEM) (Figure 2b–e), with which the highly porous structure (with both meso- and macropores) constructed by short fibre-like building blocks was observed. On the contrary, PTEB xerogels, i.e., the product obtained by conventional vacuum drying, showed a distinct compact structure with less large pores. The formation of meso- and macropores in the freeze-dried sample was due to the remaining vacancies after sublimation of the solvent. Transmission electron microscopy (TEM) images (Figure 2f,g) further revealed the existence of honeycomb-like pores at the nanometer scale for both the PTEB aerogels and the xerogels, which is consistent previous work on PTEB powder reported elsewhere.[30]

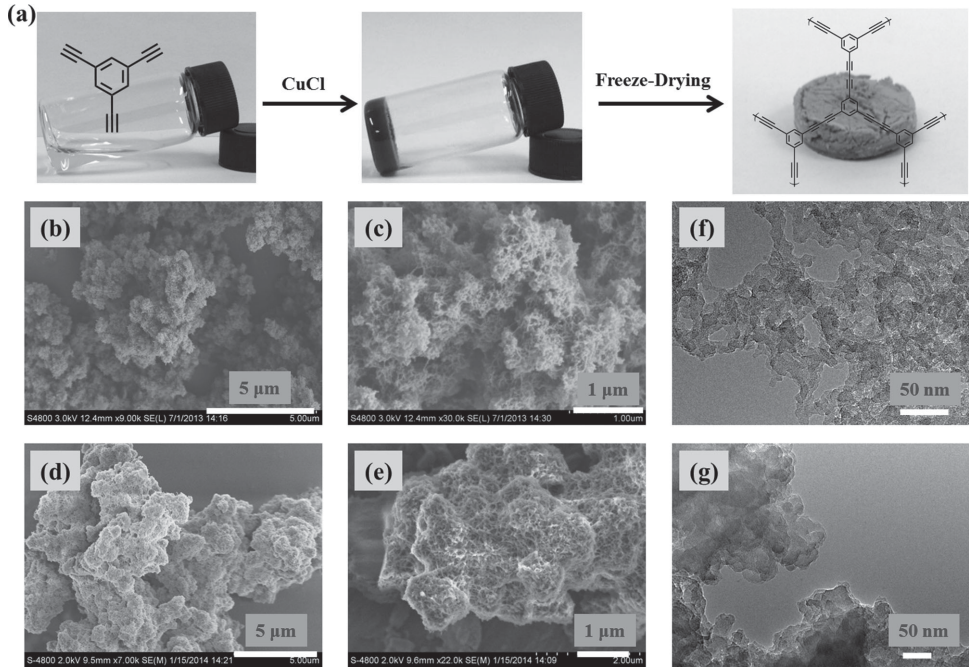

Figure 2. a) Schematic demonstration of the synthetic route toward the PTEB aerogel via Glaser coupling reactions and a following freeze-drying process. SEM images and TEM images of: b,c,f) the aerogel obtained from freeze-drying and d,e,g) the xerogel obtained from vacuum-drying.

To predict the potential for practical applications, the physical properties of the PTEB aerogels were carefully characterized. Similar to PTEB powder reported elsewhere,[30] the PTEB aerogel showed high chemical stability toward many organic solvents, and was thermally stable in a nitrogen atmosphere with weight loss less than 10 wt% up to 400 ºC (Figure S7, Supporting Information). Nitrogen adsorption measurements were adopted to evaluate the porous properties. An isothermal curve featuring both type-I and type-IV isothermal profiles was observed (**Figure 3**a),[36,37] where the steep adsorption below $p/p_0 = 0.1$ and the hysteretic loops in the high p/p_0 region are characteristics of the micro- and mesopores, respectively.[16] This hierarchical pore structure could also be unambiguously verified from the single-point pore volumes acquired at different relative pressures and pore size distribution (PSD) diagrams (Figure 3b and Table S1, Supporting Information). As shown in Table S1, by varying the formulae and the reaction conditions, the micropore's proportion could be tuned from 30% to 70%.

It is known that the freeze-drying process utilizes the sublimation of a pre-frozen solvent to avoid a huge variation of surface tension during the drying process, and thus efficiently avoiding size shrinkage and internal structure collapse. As expected, the as-obtained PTEB aerogel possessed a low density (average 30 mg cm^{-3}), thereby giving a porosity above 97%, which is characteristic of typical aerogels.[25] Notably, because of the porous structure given by the special drying process, an ultrahigh BET surface area, up to 1701 m^2 g^{-1}, was obtained, which is about 70% higher than that of both the vacuum-dried PTEB xerogel (1085 m^2 g^{-1}) and the PTEB powder (842 to 955 m^2 g^{-1}) reported elsewhere.[29,30] This value is also significantly higher than a vast number of CMPs and other MOPs (generally around 1000 m^2 g^{-1} as listed in Table S3 in the Supporting Information), although it is lower than some PAFs, COFs, and CTFs (2000–4000 m^2 g^{-1}) derived in relatively rigorous conditions.[10,11,13] Except for the enlarged surface area, the low operation temperature (currently less than 40 °C) in the freeze-drying process can also afford minimal damage towards the products. Based on the nitrogen adsorption data of the PTEB aerogels obtained under different reaction conditions (Figure S8 and Table S1, Supporting Information), the aerogel acquired with $c_0 = 15$ mg mL^{-1}, $w = 16$ wt% and $T = 40$ °C gave the best result, and was thus used for the following measurements.

Free of metal and nitrogen elements, the PTEB aerogel with exceptionally high surface area is expected to show both high capacity and reversibility simultaneously in gas adsorption. As shown in Figure 3c, the high SSA allowed the PTEB aerogel to exhibit a much higher CO_2 adsorption capacity (up to 3.47 mmol g^{-1}) than nearly all conjugated microporous polymers (typically less than 2.5 mmol g^{-1}), such as CMP-0, CMP-1, and TFM-1.[16,18,38] This value was even comparable to or better than some nitrogen/metal-containing microporous materials, which were supposed to have great adsorption capacity.[32,39] Since the CO_2 adsorption capacity of the materials linearly increases with increasing specific surface area (with similar PSD) as shown in Figure S10a in the Supporting Information, the strategy presented here is of great importance for acquiring CMP-based high-performance CO_2 adsorbents. Additionally, as illustrated in Figure 3d and Figure S9 in the Supporting Information, a considerable CH_4 adsorption capacity up to 0.913 mmol g^{-1} was also obtained. It is interestingly that the value is even higher than that of high-surface-area COF-10, COF-102 (0.36–0.67 mmol g^{-1}) and comparable to that of PAFs (0.80–1.21 mmol g^{-1}), presumably because of the appropriate pore size distribution of the PTEB aerogel.[10,11]

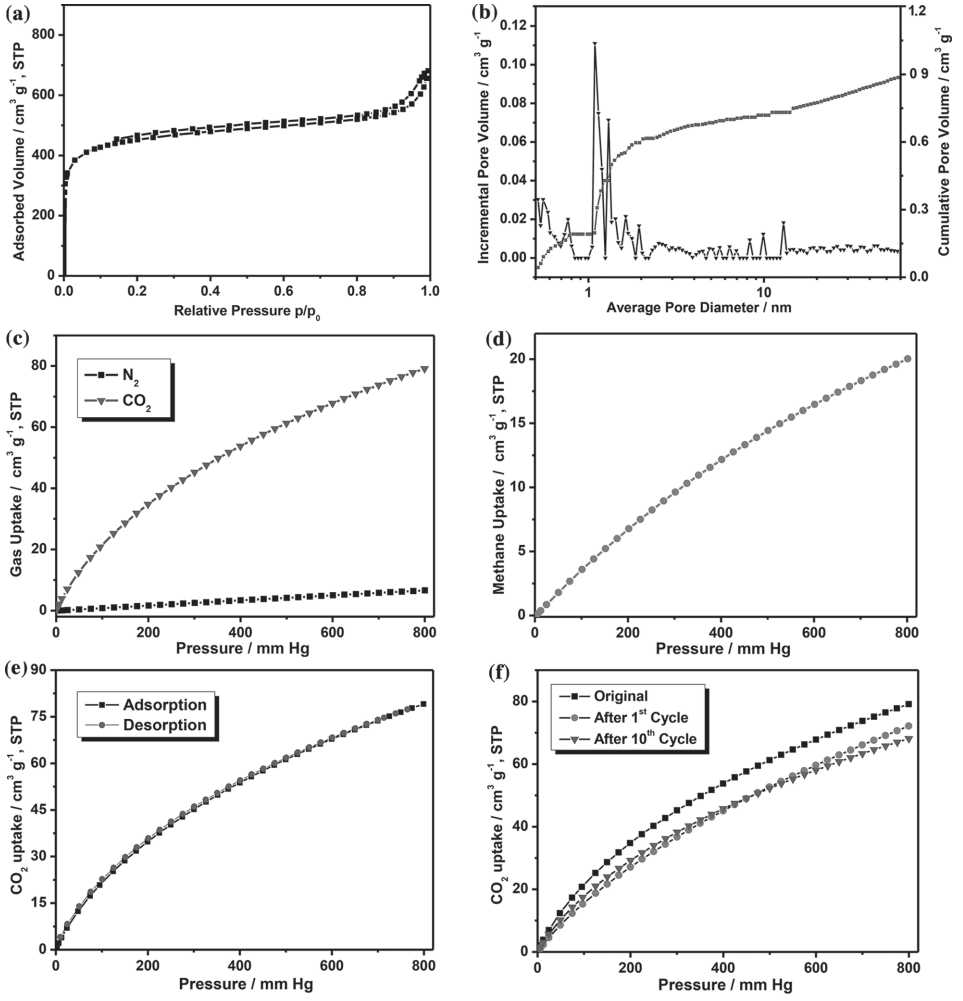

Figure 3. a) The N_2 adsorption isotherm. b) Incremental pore-size-distribution curves and cumulative pore-size-distribution curves of the PTEB aerogel. c) CO_2 and N_2 adsorption isotherms of the PTEB aerogel at 273 K. d) CH_4 adsorption isotherms of the PTEB aerogel at 273 K. e) CO_2 adsorption and desorption curves of the PTEB aerogel. f) CO_2 adsorption curves of the freshly prepared aerogel and the aerogel treated by an acetone uptake/removal process for one and ten cycles.

Selectivity is another crucial factor to evaluate the potential of a material for gas adsorption. As shown in Figure 3c, the prefered adsorption of CO_2 over N_2 revealed the remarkable selectivity of the aerogel towards these two gases. To quantitatively evaluate the selectivity, the initial slopes of the CO_2 and N_2 adsorption isotherms were compared, and the obtained selectivity of 41.2 is comparable to that of nitrogen-doped microporous materials, and considerably higher than that of nitrogen-doped polyimine-based carbons.[40,41] As a widely accepted method to estimate selective gas adsorption in a binary mixture from experimental single-component isotherms,[42] the ideal adsorption solution theory (IAST) model was adopted, with an equilibrium partial pressure of 0.85 bar for N_2 and 0.15 bar for CO_2. The CO_2 adsorption selectivity over N_2 was calculated to be 25.9, slightly higher than that of imine-linked porous polymer frameworks (14.5–20.4).[43]

Unlike nitrogen/metal-containing microporous materials, the PTEB aerogel showed a pure physical adsorption nature, and thus possesses a fully reversible adsorption/desorption process. This can be evidenced from Figure 3e, where the desorption and adsorption branches in the CO_2 isotherm curve completely overlap. Compared with polyamine-tethered porous polymer networks,[44] this reversible adsorption/desorption behavior allowed the regeneration of adsorbents with much lower energy input. Moreover, the aerogel also possessed fabulous stability, as no obvious deterioration in CO_2 capture was observed after exposure to air for several weeks (Figure S10b, Supporting Information).

In virtue of the π-conjugated backbones and high SSA, the PTEB aerogel can scavenge dye-stuffs efficiently. As shown in Figure S11 in the Supporting Information, high adsorption capacities toward both basic fuchsine (BF) (790 mg g^{-1}) and methyl blue (MB) (716 mg g^{-1}) were obtained, outperforming previously reported functional CMPs, conducting polymers, and dendrimer-linked multi-walled carbon-nanotube (MWCNT) aerogels (ca. 100–300 mg g^{-1}).[19,24,45]

On the other hand, the high organic solvent tolerance, low density, hierarchical interconnected pore structure, and monolithic form enabled the aerogel to be an excellent recyclable oil adsorbent with a large adsorption capacity and fast adsorption

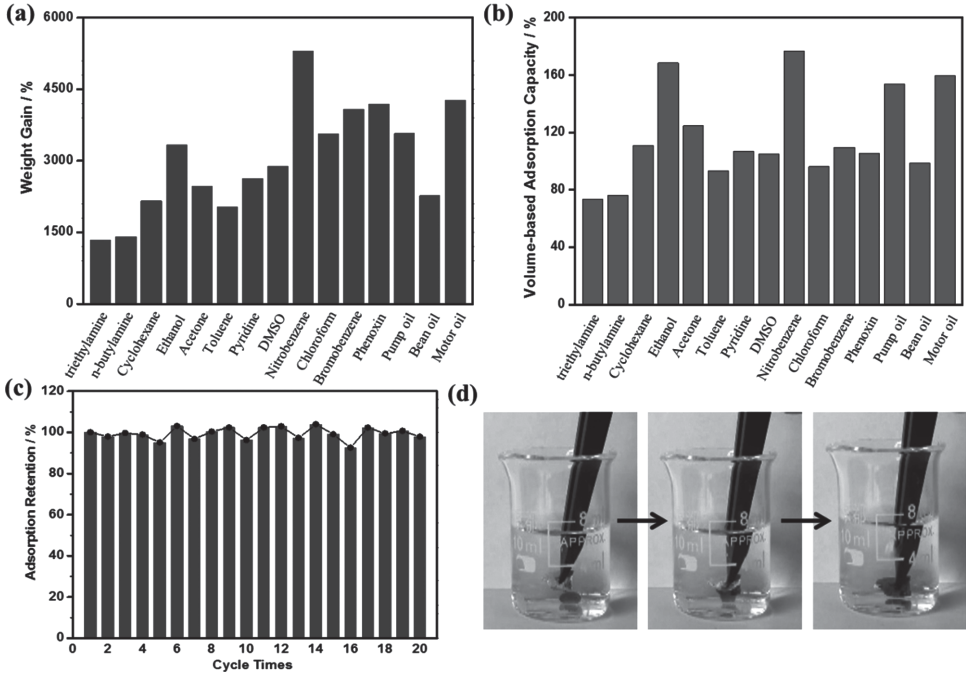

Figure 4. a,b) Mass-based (a) and volume-based (b) adsorption capacity of the PTEB aerogel. c) Adsorption-capacity retention of the PTEB aerogel toward acetone through regeneration by heating at 60 °C for 20 cycles. d) Demonstration of uptake of chloroform (dyed by Sudan III) under water, by using a piece of PTEB aerogel.

kinetics. As illustrated in **Figure 4**a, except for amines, the adsorption capacity of the aerogel towards diverse organic solvents and oils ranged from 20 to 53 times its own weight, considerably higher than that of homocoupled conjugated microporous polymer (HCMP) networks (1–16 times), porous covalent porphyrin frameworks (14.7–25.9 times) and nanoporous polydivinylbenzene (PDVB) (8–16 times) (see Table S4, Supporting Information).[46–48] Although the amine-uptake capacity of the PTEB aerogel was relatively low (13–15 times) compared with other solvents, it is still very competitive toward porphyrin-integrated CMPs (<6 times weight gain for amines).[49] On the other hand, the volume-based adsorption capacity of the PTEB aerogels ranged from 70 to 160 vol% (Figure 4b). This value is similar to that of high-adsorption-capacity carbonaceous aerogels such as carbon nanotube (CNT) sponges and N-doped graphene frameworks,[50,51] indicating the efficient space utilization of the PTEB aerogel.

More importantly, the saturated PTEB aerogel can be regenerated simply by heating in air after adsorption. As shown in Figure 4c, there is nearly no deterioration of the adsorption capacity, even after twenty acetone adsorption–regeneration cycles, indicating the amazing recyclability of the aerogel, similar to porous covalent porphyrin frameworks.[47] It is surprising that oil-uptake capacity showed no obvious changes with the change of porous structure after adsorption/desorption cycles (Table S1, Supporting Information). This suggests that the pore volume and the specific surface area might not be the only factors determining the oil sorption. The detailed mechanism for this phenomenon will be investigated in future work. Interestingly, despite the decreased pore volumes and BET surface areas on heat treatment, the regenerated aerogel maintained over 85% adsorption capacity (3.0 mmol g^{-1}) for CO_2 capture even after the acetone adsorption/desorption process for 10 cycles (Figure 3f, and Table S1,S2, Supporting Information). This means that the aerogel could be alternatively used as oil and gas adsorbents and truly serves as one of the most promising multifunctional materials.

Additionally, the free-standing PTEB aerogel can be directly used as adsorbent without any support. Along with the high hydrophobicity of PTEB because of, theoretically exclusive, carbon and hydrogen atoms included, the aerogel can maintain its adsorption efficiency in a water/oil system and be directly used for selective oil uptake. Taking chloroform as an example, this high-density toxic organic solvent could be easily removed within seconds by a piece of aerogel adsorbing it underwater (Figure 4d). The fast adsorption kinetics can be attributed to the enhancement of mass transfer from the interconnected hierarchical pores in the aerogels.

To summarize, the concept of CMP aerogels has been proposed to obtain CMP-based materials that have ultrahigh specific surface area and hierarchical pores in a general and facile way. As an example, poly(1,3,5-triethynylbenzene) aerogels were prepared by a conducting Glaser-coulping reaction under very mild conditions under an air atmosphere. The strategy used here for the preparation of the PTEB aerogel may make a step forward in integrating synthetic organic chemistry with material preparation, and thus facilitate the accessibility of CMP-based materials to a wide community of researchers. Combining the features of both CMPs and aerogels, the resultant materials showed a high porosity (ca. 97%) and an ultrahigh specific surface area (1701 m^2 g^{-1}) about 70% greater than conventional PTEB powders. Hence, despite a simple and low-cost preparation method being implemented, the resulting PTEB aerogel not only showed impressive gas-adsorption ability

toward both CO_2 and CH_4, outperforming most reported CMPs, but also exhibited promising performance as one of the most efficient recyclable adsorbents for organic pollution among all MOPs. We expect that the fusion of CMPs and aerogels may open new opportunities to create a class of novel porous and high-performance materials suitable for a variety of practical applications in gas-adsorption, oil-uptake, light-harvesting, and energy-related fields.

Experimental Section

Preparation of the CMP Organogel and Aerogel: Typically, 1,3,5-triethynylbenzene (30 mg, 0.2 mmol) and CuCl (6 mg, 0.06 mmol) were dissolved in pyridine (2 mL) in a glass bottle. The bottle was then sealed and subjected to heating in a water bath at 40 °C for 72 h. The product was washed with a variety of organic solvents. Finally, the solvent inside the gel was exchanged with water or tert-butyl alcohol, and the PTEB aerogel was obtained by freeze-drying for 24 h. The detailed conditions are described in the Supporting Information.

Supporting Information

Supporting Information is available from the Wiley Online Library or from the author.

Acknowledgements

This work was supported by the NSFC (21233001, 21129001, 51272006, 51121091 and 51432002) and MOST (2011CB932601).

Received: July 9, 2014
Revised: September 11, 2014
Published online: October 22, 2014

[1] J. X. Jiang, F. Su, A. Trewin, C. D. Wood, N. L. Campbell, H. Niu, C. Dickinson, A. Y. Ganin, M. J. Rosseinsky, Y. Z. Khimyak, *Angew. Chem. Int. Ed.* **2007**, *46*, 8574.
[2] A. I. Cooper, *Adv. Mater.* **2009**, *21*, 1291.
[3] Y. Xu, S. Jin, H. Xu, A. Nagai, D. Jiang, *Chem. Soc. Rev.* **2013**, *42*, 8012.
[4] F. Vilela, K. Zhang, M. Antonietti, *Energy Environ. Sci.* **2012**, *5*, 7819.
[5] Z. Chang, D.-S. Zhang, Q. Chen, X.-H. Bu, *Phys. Chem. Chem. Phys.* **2013**, *15*, 5430.
[6] R. Dawson, A. I. Cooper, D. J. Adams, *Prog. Polym. Sci.* **2012**, *37*, 530.
[7] Y. Kou, Y. Xu, Z. Guo, D. Jiang, *Angew. Chem. Int. Ed.* **2011**, *50*, 8753.
[8] L. Chen, Y. Honsho, S. Seki, D. Jiang, *J. Am. Chem. Soc.* **2010**, *132*, 6742.
[9] Y. Xu, L. Chen, Z. Guo, A. Nagai, D. Jiang, *J. Am. Chem. Soc.* **2011**, *133*, 17622.
[10] H. Furukawa, O. M. Yaghi, *J. Am. Chem. Soc.* **2009**, *131*, 8875.
[11] T. Ben, C. Pei, D. Zhang, J. Xu, F. Deng, X. Jing, S. Qiu, *Energy Environ. Sci.* **2011**, *4*, 3991.
[12] J.-X. Jiang, F. Su, A. Trewin, C. D. Wood, H. Niu, J. T. Jones, Y. Z. Khimyak, A. I. Cooper, *J. Am. Chem. Soc.* **2008**, *130*, 7710.
[13] P. Kuhn, M. Antonietti, A. Thomas, *Angew. Chem. Int. Ed.* **2008**, *47*, 3450.
[14] B. G. Hauser, O. K. Farha, J. Exley, J. T. Hupp, *Chem. Mater.* **2012**, *25*, 12.
[15] N. Kobayashi, M. Kijima, *J. Mater. Chem.* **2007**, *17*, 4289.
[16] S. Ren, R. Dawson, A. Laybourn, J.-x. Jiang, Y. Khimyak, D. J. Adams, A. I. Cooper, *Polym. Chem.* **2012**, *3*, 928.
[17] A. Li, R. F. Lu, Y. Wang, X. Wang, K. L. Han, W. Q. Deng, *Angew. Chem. Int. Ed.* **2010**, *49*, 3330.
[18] X. Zhu, C. Tian, S. M. Mahurin, S.-H. Chai, C. Wang, S. Brown, G. M. Veith, H. Luo, H. Liu, S. Dai, *J. Am. Chem. Soc.* **2012**, *134*, 10478.
[19] A. P. Nelson, O. K. Farha, K. L. Mulfort, J. T. Hupp, *J. Am. Chem. Soc.* **2009**, *131*, 458.
[20] H. F. Zhang, I. Hussain, M. Brust, M. F. Butler, S. P. Rannard, A. I. Cooper, *Nat. Mater.* **2005**, *4*, 787.
[21] R. Du, X. Zhang, *Acta Physico-Chimica Sinica* **2012**, *28*, 2305.
[22] R. Du, Y. Xu, Y. Luo, X. Zhang, J. Zhang, *Chem. Commun.* **2011**, *47*, 6287.
[23] R. Du, J. Wu, L. Chen, H. Huang, X. Zhang, J. Zhang, *Small* **2014**, *10*, 1387.
[24] X. Zhang, L. Chen, T. Yuan, H. Huang, Z. Sui, R. Du, X. Li, Y. Lu, Q. Li, *Mater. Horiz.* **2014**, *1*, 232.
[25] A. C. Pierre, G. M. Pajonk, *Chem. Rev.* **2002**, *102*, 4243.
[26] F. Franks, *Eur. J. Pharm. Biopharm.* **1998**, *45*, 221.
[27] S. Nardecchia, D. Carriazo, M. L. Ferrer, M. C. Gutierrez, F. del Monte, *Chem. Soc. Rev.* **2013**, *42*, 794.
[28] A. S. Hay, *J. Org. Chem.* **1962**, *27*, 3320.
[29] J.-X. Jiang, F. Su, H. Niu, C. D. Wood, N. L. Campbell, Y. Z. Khimyak, A. I. Cooper, *Chem. Commun.* **2008**, 486.
[30] A. Li, H.-X. Sun, D.-Z. Tan, W.-J. Fan, S.-H. Wen, X.-J. Qing, G.-X. Li, S.-Y. Li, W.-Q. Deng, *Energy Environ. Sci.* **2011**, *4*, 2062.
[31] C. D. Wood, B. Tan, A. Trewin, F. Su, M. J. Rosseinsky, D. Bradshaw, Y. Sun, L. Zhou, A. I. Cooper, *Adv. Mater.* **2008**, *20*, 1916.
[32] P. Mohanty, L. D. Kull, K. Landskron, *Nat. Commun.* **2011**, *2*, 401.
[33] P. Arab, M. G. Rabbani, A. K. Sekizkardes, T. Islamoglu, H. M. El-Kaderi, *Chem. Mater.* **2014**, *26*, 1385.
[34] G. Li, Y. Li, H. Liu, Y. Guo, Y. Li, D. Zhu, *Chem. Commun.* **2010**, *46*, 3256.
[35] M. J. Schultz, X. Zhang, S. Unarunotai, D.-Y. Khang, Q. Cao, C. Wang, C. Lei, S. MacLaren, J. A. Soares, I. Petrov, *Proc. Natl. Acad. Sci. USA* **2008**, *105*, 7353.
[36] K. Sing, D. Everett, R. Haul, L. Moscou, R. Pierotti, J. Rouquerol, T. Siemieniewska, *Pure Appl. Chem* **1982**, *54*, 2201.
[37] R. Kumar, V. M. Suresh, T. K. Maji, C. Rao, *Chem. Commun.* **2014**, *50*, 2015.
[38] R. Dawson, D. J. Adams, A. I. Cooper, *Chem. Sci.* **2011**, *2*, 1173.
[39] H. Ma, H. Ren, X. Zou, S. Meng, F. Sun, G. Zhu, *Polym. Chem.* **2014**, *5*, 144.
[40] J. Wei, D. Zhou, Z. Sun, Y. Deng, Y. Xia, D. Zhao, *Adv. Funct. Mater.* **2013**, *23*, 2322.
[41] J. Wang, I. Senkovska, M. Oschatz, M. R. Lohe, L. Borchardt, A. Heerwig, Q. Liu, S. Kaskel, *J. Mater. Chem. A* **2013**, *1*, 10951.
[42] C. Xu, N. Hedin, *J. Mater. Chem. A* **2013**, *1*, 3406.
[43] Y. Zhu, H. Long, W. Zhang, *Chem. Mater.* **2013**, *25*, 1630.
[44] W. Lu, J. P. Sculley, D. Yuan, R. Krishna, Z. Wei, H. C. Zhou, *Angew. Chem. Int. Ed.* **2012**, *51*, 7480.
[45] R. Dawson, A. Laybourn, R. Clowes, Y. Z. Khimyak, D. J. Adams, A. I. Cooper, *Macromolecules* **2009**, *42*, 8809.
[46] D. Tan, W. Fan, W. Xiong, H. Sun, A. Li, W. Deng, C. Meng, *Eur. Polym. J.* **2012**, *48*, 705.
[47] X.-S. Wang, J. Liu, J. M. Bonefont, D.-Q. Yuan, P. K. Thallapally, S. Ma, *Chem. Commun.* **2013**, *49*, 1533.
[48] Y. Zhang, S. Wei, F. Liu, Y. Du, S. Liu, Y. Ji, T. Yokoi, T. Tatsumi, F.-S. Xiao, *Nano Today* **2009**, *4*, 135.
[49] X. Liu, Y. Xu, Z. Guo, A. Nagai, D. Jiang, *Chem. Commun.* **2013**, *49*, 3233.
[50] X. Gui, J. Wei, K. Wang, A. Cao, H. Zhu, Y. Jia, Q. Shu, D. Wu, *Adv. Mater.* **2010**, *22*, 617.
[51] Y. Zhao, C. Hu, Y. Hu, H. Cheng, G. Shi, L. Qu, *Angew. Chem.* **2012**, *124*, 11533.